Tm:KLu(WO$_4$)$_2$ microchip laser Q-switched by a graphene-based saturable absorber

Josep Maria Serres,[1] Pavel Loiko,[1,2] Xavier Mateos,[1,*] Konstantin Yumashev,[2] Uwe Griebner,[3] Valentin Petrov,[3] Magdalena Aguiló,[1] and Francesc Díaz[1]

[1]*Física i Cristal·lografia de Materials i Nanomaterials (FiCMA-FiCNA), Universitat Rovira i Virgili (URV), Campus Sescelades, c/ Marcel·lí Domingo, s/n., Tarragona, E-43007, Spain*

[2]*Center for Optical Materials and Technologies, Belarusian National Technical University, 65/17 Nezavisimosti Ave., Minsk, 220013, Belarus*

[3]*Max Born Institute for Nonlinear Optics and Short Pulse Spectroscopy, 2A Max-Born-Str., Berlin, D-12489, Germany*

*xavier.mateos@urv.cat

Abstract: We report on the first Tm-doped double tungstate microchip laser Q-switched with graphene using a Tm:KLu(WO$_4$)$_2$ crystal cut along the N_g dielectric axis. This laser generates a maximum average output power of 310 mW with a slope efficiency of 13%. At a repetition rate of 190 kHz the shortest pulses with 285 ns duration and 1.6 μJ energy are achieved.

OCIS codes: (140.3480) Lasers, diode-pumped; (140.3540) Lasers, Q-switched.

References and links

1. R. C. Stoneman and L. Esterowitz, "Efficient, broadly tunable, laser-pumped Tm:YAG and Tm:YSGG cw lasers," Opt. Lett. **15**(9), 486–488 (1990).
2. V. Petrov, M. C. Pujol, X. Mateos, O. Silvestre, S. Rivier, M. Aguilo, R. M. Sole, J. H. Liu, U. Griebner, and F. Diaz, "Growth and properties of KLu(WO$_4$)$_2$, and novel ytterbium and thulium lasers based on this monoclinic crystalline host," Laser Photon. Rev. **1**(2), 179–212 (2007).
3. S. N. Bagaev, S. M. Vatnik, A. P. Maiorov, A. A. Pavlyuk, and D. V. Plakushchev, "The spectroscopy and lasing of monoclinic Tm:KY(WO$_4$)$_2$ crystals," Quantum Electron. **30**(4), 310–314 (2000).
4. A. E. Troshin, V. E. Kisel, A. S. Yasukevich, N. V. Kuleshov, A. A. Pavlyuk, E. B. Dunina, and A. A. Kornienko, "Spectroscopy and laser properties of Tm:KY(WO$_4$)$_2$ crystal," Appl. Phys. B **86**(2), 287–292 (2007).
5. O. Silvestre, M. C. Pujol, M. Rico, F. Güell, M. Aguiló, and F. Díaz, "Thulium doped monoclinic KLu(WO$_4$)$_2$ single crystals: growth and spectroscopy," Appl. Phys. B **87**(4), 707–716 (2007).
6. P. A. Loiko, S. M. Vatnik, I. A. Vedin, A. A. Pavlyuk, K. V. Yumashev, and N. V. Kuleshov, "Thermal lensing in N_m-cut monoclinic Tm:KLu(WO$_4$)$_2$ laser crystal," Laser Phys. Lett. **10**(12), 125005 (2013).
7. X. Mateos, V. Petrov, J. Liu, M. C. Pujol, U. Griebner, M. Aguilo, F. Diaz, M. Galan, and G. Viera, "Efficient 2-μm continuous-wave laser oscillation of Tm^{3+}:KLu(WO$_4$)$_2$," IEEE J. Quantum Electron. **42**, 1008–1015 (2006).
8. S. M. Vatnik, I. A. Vedin, and A. A. Pavlyuk, "High-efficiency 5% Tm:KLu(WO$_4$)$_2$ N_m-cut minislab laser," Laser Phys. Lett. **9**(11), 765–769 (2012).
9. M. Segura, M. Kadankov, X. Mateos, M. C. Pujol, J. J. Carvajal, M. Aguiló, F. Díaz, U. Griebner, and V. Petrov, "Passive Q-switching of the diode pumped Tm^{3+}:KLu(WO$_4$)$_2$ laser near 2-μm with Cr^{2+}:ZnS saturable absorbers," Opt. Express **20**(4), 3394–3400 (2012).
10. M. S. Gaponenko, I. A. Denisov, V. E. Kisel, A. M. Malyarevich, A. A. Zhilin, A. A. Onushchenko, N. V. Kuleshov, and K. V. Yumashev, "Diode-pumped Tm:KY(WO$_4$)$_2$ laser passively Q-switched with PbS-doped glass," Appl. Phys. B **93**(4), 787–791 (2008).
11. A. Schmidt, S. Y. Choi, D. Il Yeom, F. Rotermund, X. Mateos, M. Segura, F. Diaz, V. Petrov, and U. Griebner, "Femtosecond pulses near 2 μm from a Tm:KLuW laser mode-locked by a single-walled carbon nanotube saturable absorber," Appl. Phys. Express **5**(9), 092704 (2012).
12. A. A. Lagatsky, S. Calvez, J. A. Gupta, V. E. Kisel, N. V. Kuleshov, C. T. A. Brown, M. D. Dawson, and W. Sibbett, "Broadly tunable femtosecond mode-locking in a Tm:KYW laser near 2 μm," Opt. Express **19**(10), 9995–10000 (2011).
13. A. K. Geim and K. S. Novoselov, "The rise of graphene," Nat. Mater. **6**(3), 183–191 (2007).
14. Q. Bao, H. Zhang, Y. Wang, Z. Ni, Y. Yan, Z. X. Shen, K. P. Loh, and D. Y. Tang, "Atomic-layer graphene as a saturable absorber for ultrafast pulsed lasers," Adv. Funct. Mater. **19**(19), 3077–3083 (2009).
15. Q. Bao, H. Zhang, Z. Ni, Y. Wang, L. Polavarapu, Z. Shen, Q. H. Xu, D. Y. Tang, and K. P. Loh, "Monolayer graphene as saturable absorber in mode-locked laser," Nano Res. **4**(3), 297–307 (2011).
16. G. Xing, H. Guo, X. Zhang, T. C. Sum, and C. H. A. Huan, "The Physics of ultrafast saturable absorption in graphene," Opt. Express **18**(5), 4564–4573 (2010).

#236206 - $15.00 USD Received 13 Mar 2015; revised 9 May 2015; accepted 11 May 2015; published 20 May 2015

17. Q. Wang, H. Teng, Y. Zou, Z. Zhang, D. Li, R. Wang, C. Gao, J. Lin, L. Guo, and Z. Wei, "Graphene on SiC as a Q-switcher for a 2 μm laser," Opt. Lett. **37**(3), 395–397 (2012).
18. G. Q. Xie, J. Ma, P. Lv, W. L. Gao, P. Yuan, L. J. Qian, H. H. Yu, H. J. Zhang, J. Y. Wang, and D. Y. Tang, "Graphene saturable absorber for Q-switching and mode locking at 2 μm wavelength," Opt. Mater. Express **2**(6), 878–883 (2012).
19. T. L. Feng, S. Z. Zhao, K. J. Yang, G. Q. Li, D. C. Li, J. Zhao, W. C. Qiao, J. Hou, Y. Yang, J. L. He, L. H. Zheng, Q. G. Wang, X. D. Xu, L. B. Su, and J. Xu, "Diode-pumped continuous wave tunable and graphene Q-switched Tm:LSO lasers," Opt. Express **21**(21), 24665–24673 (2013).
20. T. Zhao, Y. Wang, H. Chen, and D. Shen, "Graphene passively Q-switched Ho:YAG ceramic laser," Appl. Phys. B **116**(4), 947–950 (2014).
21. C. J. Jin, X. M. Chen, L. F. Li, M. Qi, Y. Bai, Z. Y. Ren, and J. T. Bai, "A graphene-based passively Q-switched Ho:YAG laser in-band pumped by a diode-pumped Tm:YLF solid-state laser," Laser Phys. **24**(3), 035801 (2014).
22. B. Q. Yao, Z. Cui, X. M. Duan, Y. J. Shen, J. Wang, and Y. Q. Du, "A graphene-based passively Q-switched Ho:YAG laser," Chin. Phys. Lett. **31**(7), 074204 (2014).
23. Z. Cui, B. Yao, X. Duan, Y. Du, S. Xu, and Y. Wang, "Stable passively Q-switched Ho:LuAG laser with graphene as a saturable absorber," Opt. Eng. **53**(12), 126112 (2014).
24. U. Griebner, J. M. Serres, X. Mateos, V. Petrov, M. Aguiló, and F. Díaz, "Graphene saturable absorber Q-switched Tm:$KLu(WO_4)_2$ laser emitting at 2 μm," Advanced Solid-State Lasers (ASSL) 2014, paper ATh2A.16.
25. J. J. Zayhowski and A. Mooradian, "Single-frequency microchip Nd lasers," Opt. Lett. **14**(1), 24–26 (1989).
26. M. S. Gaponenko, P. A. Loiko, N. V. Gusakova, K. V. Yumashev, N. V. Kuleshov, and A. A. Pavlyuk, "Thermal lensing and microchip laser performance of N_g-cut Tm^{3+}:$KY(WO_4)_2$ crystal," Appl. Phys. B **108**(3), 603–607 (2012).
27. J. M. Serres, X. Mateos, P. Loiko, K. Yumashev, N. Kuleshov, V. Petrov, U. Griebner, M. Aguiló, and F. Díaz, "Diode-pumped microchip Tm:$KLu(WO_4)_2$ laser with more than 3 W of output power," Opt. Lett. **39**(14), 4247–4250 (2014).
28. P. A. Loiko, J. M. Serres, X. Mateos, K. V. Yumashev, N. V. Kuleshov, V. Petrov, U. Griebner, M. Aguiló, and F. Díaz, "Characterization of thermal lens in Tm:$KLu(WO_4)_2$ and microchip laser operation," Laser Phys. Lett. **11**(7), 075001 (2014).
29. A. A. Balandin, S. Ghosh, W. Bao, I. Calizo, D. Teweldebrhan, F. Miao, and C. N. Lau, "Superior thermal conductivity of single-layer graphene," Nano Lett. **8**(3), 902–907 (2008).
30. D. Yoon, Y. W. Son, and H. Cheong, "Negative thermal expansion coefficient of graphene measured by Raman spectroscopy," Nano Lett. **11**(8), 3227–3231 (2011).
31. F. Zhang, S. Han, Y. Liu, Z. Wang, and X. Xu, "Dependence of the saturable absorption of graphene upon excitation photon energy," Appl. Phys. Lett. **106**(9), 091102 (2015).

1. Introduction

Lasers emitting near 2 μm are of practical importance for medicine (as several absorption bands of water fall into this spectral region), remote sensing of CO_2 and water in the atmosphere (LIDAR applications) and pumping of mid-IR optical parametric oscillators (OPOs). Typically, such lasers are based on trivalent holmium, Ho^{3+}, or thulium, Tm^{3+}, ions. The benefits of Tm-doped materials are the efficient pumping with commercial AlGaAs laser diodes around 794–802 nm ($^3H_6 \rightarrow {}^3H_4$ transition), as well as enhanced laser efficiency due to several cross-relaxation (CR) processes [1]. Tm lasers can also be used for in-band pumping of Ho laserss, with the prospect to shift the laser wavelength up to 2.1 μm.

Monoclinic double tungstates (DTs), $KRE(WO_4)_2$ or shortly KREW where RE denotes a passive element like Y, Gd or Lu, have been intensively studied in recent years as Tm-hosts [2]. Among them, potassium luthetium tungstate, KLuW, is the best solution in terms of proper matching between ionic radii of eight-fold coordinated Lu^{3+} and Tm^{3+} ions (0.977 and 0.994 Å, respectively). This means high Tm content and efficient CR maintaining an excellent crystal quality. In addition, Tm:DTs offer intense and wide absorption and stimulated-emission bands with a strong polarization-anisotropy [3–5]. Due to the CR processes, the heat loading in Tm:DTs is relatively low [6]. Highly efficient multi-watt continuous-wave (CW) [7,8], Q-switched [9,10] and fs mode-locked [11,12] Tm:KREW lasers were realized recently.

Passive Q-switching (PQS) of diode-pumped Tm:KLuW and Tm:KYW lasers was realized with Cr^{2+}-doped ZnS [9] and PbS quantum-dot-doped glass [10]. Graphene, a single atomic carbon layer [13], is emerging as ultra-broadband saturable absorber (SA) for the near-IR with beneficial properties including high optical transparency, ultrafast saturable absorption, fast recovery time and moderate modulation depth [14–16]. Bulk Nd-, Yb- and Er-lasers Q-switched with graphene were intensively studied during the last decade; however, only few implementations of graphene SA in 2 μm bulk lasers are known. These include

#236206 - $15.00 USD Received 13 Mar 2015; revised 9 May 2015; accepted 11 May 2015; published 20 May 2015

Tm:YAG with double-layer graphene on SiC [17], and Tm:CLNGG and Tm:LSO lasers with graphene layer deposited on Cu as a SA mirror [18,19]. In these reports, μs-long pulse durations were achieved at relatively low output power, see summary of output characteristics in Table 1. Q-switching of Ho bulk lasers with graphene was reported in [20–23].

Table 1. Summary of graphene Q-switched bulk lasers around ~2 μm reported so far.

Gain material	P_{out}, mW	τ, μs	PRF, kHz	E_{out}, μJ	Ref.
Tm:CLNGG	40	9	5.8	6.9	[17]
Tm:YAG	38	2.08	18.1	1.74	[18]
Tm:LSO	106	7.8	7.6	14	[19]
Tm:KLuW	34	3.7	39	1	[24]
Ho:YAG ceramics	264	9	64	9.3	[20]
Ho:YAG	572	0.63	43	13.3	[21]
Ho:YAG	100	2.11	57.1	1.75	[22]
Ho:LuAG	370	0.78	47.3	7.8	[23]

P_{out} is the average output power; τ is the pulse duration;
PRF is the pulse repetition frequency; E_{out} is the pulse energy

In the present paper, our goal was to realize a Tm:KLuW microchip laser Q-switched by a graphene SA. The microchip concept has a high potential in terms of low losses, compact design, improved cooling, low sensitivity to misalignment, and, hence, higher laser efficiency and output power compared to conventional two mirror resonators [25]. It was shown that Tm:DTs are suitable for the monolithic laser concept [26,27], provided a special crystal cut for light propagation along the N_g dielectric axis is chosen. For this cut, the desired mode stabilization in the plano-plano cavity is ensured by a positive and nearly spherical thermal lens [28]; these properties are not available for the crystal cut along the growth direction, the *b*-axis. The specific features of the microchip concept allowed us to achieve ~10-fold improvement in terms of output power and pulse duration as compared with a recent report on Tm:KLuW laser with a hemispherical cavity Q-switched with a graphene SA [24].

2. Experimental

The studied laser crystal, 3 at.% Tm:KLuW, was grown by the Top-Seeded-Solution Growth (TSSG) slow-cooling method. From the as-grown bulk, a 2.60 mm-thick rectangular sample was cut along the N_g optical indicatrix axis. Both $m \times p$ faces of the crystal with dimensions 3 × 3 mm^2 were polished to laser quality and antireflection (AR) coated for the 1.80–2.08 μm range. The crystal was mounted in a Cu-holder providing cooling from all four lateral sides and Indium foil ensured good thermal contact. The holder was water-cooled down to 12°C.

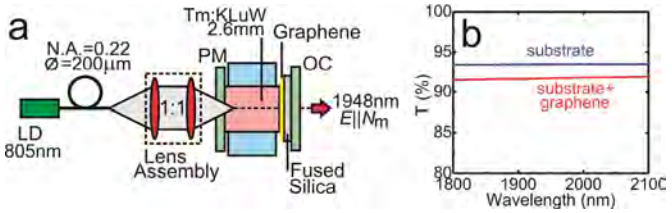

Fig. 1. (a) Set-up of the graphene SA passively Q-switched Tm:KLuW microchip laser; (b) Transmission of the graphene SA as compared with a pure fused silica substrate.

The plano-plano cavity of the microchip laser, Fig. 1(a), consisted of a pump mirror (PM) AR-coated for 0.77–1.05 μm and high-reflection (HR) coated for 1.80–2.08 μm, and an output coupler (OC) with transmittance T_{OC} = 5% at the laser wavelength. The PM was attached directly to the polished crystal face without an air gap. Between the second face of the crystal and OC, a commercial transmission-type graphene-based SA was inserted. The graphene SA consisted of a 1.05 mm-thick fused silica substrate with a single-layer graphene deposited by chemical vapor deposition (CVD). Its initial transmission at the laser wavelength was 97.8%, see Fig. 1(b). This agrees well with the universal transmission of a single-layer graphene, $T = 1 - \pi\alpha \approx 97.7\%$ (where α is the fine structure constant). The characterization of this sample

#236206 - $15.00 USD Received 13 Mar 2015; revised 9 May 2015; accepted 11 May 2015; published 20 May 2015

with Raman spectroscopy indicates a ratio of the integrated areas of 2D and G bands of ~4, confirming the presence of a single carbon layer [24]. Both SA and PM were also attached without air gaps, thus providing a total geometrical cavity length of 3.65 mm. The radius of the laser mode on the graphene SA for the "hot" cavity was ~70 μm.

As a pump source we employed an AlGaAs fiber coupled laser diode (LD, fiber core diameter: 200 μm, numerical aperture N.A.: 0.22) temperature-tuned to ~805 nm. The unpolarized pump radiation was collimated and focused into the crystal using a lens assembly (1:1 imaging ratio, 30 mm focal length) resulting in a pump spot radius w_p in the crystal of ~100 μm. The confocal parameter for the pump system was $2z_R$ ~3.0 mm. No pump bleaching of the crystal absorption was observed. The measured single-pass absorption in the crystal was 62% while the SA absorbed about 3.2% of the residual pump light at 805 nm.

3. Results and discussion

Output coupler with TOC = 5% was selected because in a preliminary experiment using a hemispherical cavity, we investigated OCs with transmittance of 3, 5, 9 and 15%. Stable PQS was achieved only for TOC = 5% and 9% with similar results on the output power [24]. However, 5% OC provided better stability and repeatability of the pulse train, as well as allowed wider range of pump power where PQS was observed. This behavior was confirmed for the microchip cavity.

Very stable PQS of the Tm:KLuW microchip laser was achieved for absorbed powers P_{abs} in the range 1.1–3.3 W. The maximum average output power amounted to 310 mW with a slope efficiency of 13%, Fig. 2(a). The laser threshold was relatively low, ~0.9 W. For P_{abs} >3.3 W, PQS was detected but it was impossible to stabilize the laser. Without SA in the cavity, the CW output power was 1.55 W at P_{abs} = 3.3 W with a slope efficiency of 56%. Thus, the conversion efficiency from CW to Q-switched regime was 24%. The CW laser threshold was ~0.55 W. A linear behavior of the input-output curve, as shown in Fig. 2(a), clearly indicates the absence of detrimental thermal effects. No damage of the graphene SA was observed. For both regimes the laser emission was linearly polarized, $E \parallel N_m$ and the laser wavelength was 1948 nm, see inset in Fig. 2(a). The emission wavelength corresponds to a local maximum in the gain spectrum of Tm:KLuW for low inversion ratios, $\beta < 0.2$ [5].

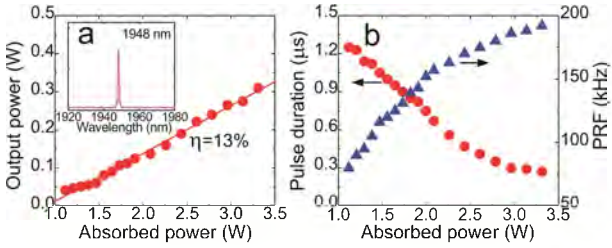

Fig. 2. Graphene SA passively Q-switched Tm:KLuW microchip laser, (a) Input-output dependence and (b) pulse duration and pulse repetition frequency (PRF) versus absorbed pump power; *inset*: typical emission spectrum for P_{abs} = 3.3 W.

Q-switching instabilities for P_{abs} >3.3 W are partially attributed to heating of the graphene SA due to residual (non-absorbed) pump. It is known that graphene possesses a very high thermal conductivity, κ ~5000 $Wm^{-1}K^{-1}$ [29] but it was deposited on a passively-cooled silica substrate with much lower thermal conductivity, κ ~1.3 $Wm^{-1}K^{-1}$, so heating of both substances is expected. When the graphene/substrate interface is heated, both materials exhibit thermal expansion. Graphene has a negative coefficient of thermal expansion (CTE), -7×10^{-6} K^{-1} [30]. For fused silica, CTE is positive, 0.5×10^{-6} K^{-1}. The CTE mismatch causes a compressive strain in the graphene layer with rising temperature and can in principle lead to its slip or buckling from the substrate surface. Thus, increased scattering on the graphene/substrate interface and spatially non-uniform increase of the non-saturable loss will be observed.

#236206 - $15.00 USD Received 13 Mar 2015; revised 9 May 2015; accepted 11 May 2015; published 20 May 2015

The unchanged laser wavelength after insertion of the SA, as well as the moderate increase of the threshold indicate that the losses introduced by the graphene SA are relatively low (a previous study yielded an estimation of ~4.4% as round-trip loss [24]). In addition, the microchip laser design itself provided low losses compared to extended two mirror cavities. This leads to a significant scaling (about 10-times) of the average output power, as compared with the previous result for the graphene Q-switched Tm:KLuW laser with a hemispherical cavity, namely 34 mW for P_{abs} = 1.07 W with a slope efficiency of 11.5% (T_{OC} = 9%) [24].

With the increase of pump power, the duration of the single Q-switched pulse (FWHM) decreased from 1.25 µs to 285 ns. This dependence began to saturate for P_{abs} > 3 W. The pulse repetition frequency (PRF) increased from 81 to 190 kHz, see Fig. 2(b). Figure 3(a) shows an oscilloscope trace of the shortest Q-switched pulse and Fig. 3(b) a typical pulse train at a repetition rate of 190 kHz, both at P_{abs} = 3.3 W. As compared with a previous report on a graphene SA Tm:KLuW laser (shortest pulse duration: 3.7 µs for T_{OC} = 5%), nearly 10-fold pulse shortening is achieved. We attribute this pulse shortening to the substantial reduction of the cavity length and the higher intracavity intensity. As a result better bleaching of the SA is achieved by (i) smaller radius of the laser mode in the microchip setup, ~70 µm (compared to the calculated value of ~210 µm for the hemispherical cavity described in [24]), and (ii) a higher pump level keeping the stability of the PQS operation, as discussed above.

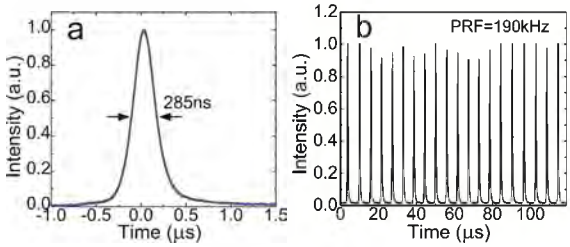

Fig. 3. Single pulse (a) and pulse train (b) records of the graphene SA passively Q-switched Tm:KLuW microchip laser; P_{abs} = 3.3 W. A fast InGaAs photodiode (rise time: 200 ps) and a 2 GHz digital oscilloscope were used for such measurements.

Figure 4 shows the temporal stability of the Q-switched Tm:KLuW microchip laser indicating amplitude fluctuations of <10%. We even extended these measurements to a time window of ~20 min and observed no degradation of the PQS laser performance.

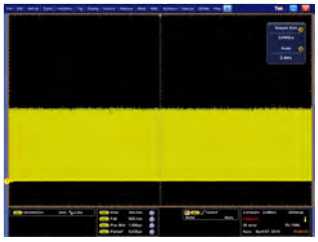

Fig. 4. Oscilloscope trace of the graphene SA passively Q-switched Tm:KLuW microchip laser at P_{abs} = 1.8 W. The total time window is 20 ms.

Figure 5(a) shows the calculated pulse energy for the Q-switched Tm:KLuW microchip laser. The pulse energy exhibits a nearly linear dependence on the absorbed pump power with the maximum of ~1.6 µJ achieved at P_{abs} = 3.3 W indicating further power scalability. The calculated intracavity intensity I for this pump power is ~2.2 MW/cm^2. For a CVD-grown single-layer graphene with a total absorbance of ~2.3%, the saturation intensity at ~1.95 µm is I_S = 0.61 MW/cm^2 and the non-saturable loss is $\Delta\alpha^*_{NS}$ ~0.8% [31]. Thus, the intensity on the graphene SA is slightly above I_S and power scaling of the microchip laser is possible when operating the graphene SA several times above I_S. The limit in our case we attribute to heating of the graphene layer as mentioned above, not to the mode size restrictions given by the microchip laser concept. For the considered I the modulation depth will be only 1.2% that is

#236206 - $15.00 USD Received 13 Mar 2015; revised 9 May 2015; accepted 11 May 2015; published 20 May 2015

below its maximum value of $\Delta\alpha^*_S$ = 1.5%. The Q-switched microchip laser corresponded to the TEM_{00} mode with excellent beam profile and $M^2_{x,y}$<1.2 (x ≡ *p*, y ≡ *m*). This is related to the low astigmatism of the thermal lens for N_g-cut Tm:KLuW crystals [28]. The peak power is shown in Fig. 5(b) with a maximum of about 6 W.

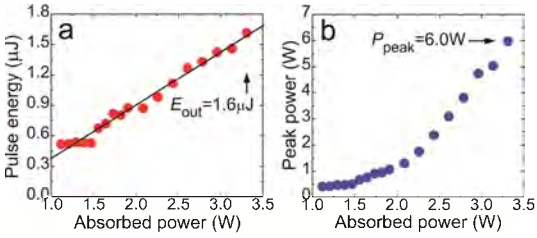

Fig. 5. Graphene SA passively Q-switched Tm:KLuW microchip laser: pulse energy (a) and peak power (b) versus absorbed pump power.

Although this study presents a substantial improvement of graphene Q-switched Tm lasers in terms of pulse duration and average output, the achieved pulse energy E_{out} ~1.6 μJ is not so high. Attention should be paid to the reduction of unwanted heating of the SA by the residual pump, e.g. by increasing the Tm content that can be easily realized in the KLuW host. For scaling to distinct larger pulse energies >100μJ a higher modulation depth is preferable. The use of single-layer graphene limits the maximum $\Delta\alpha^*_S$ value to ~1.5%. In the previous works on Tm lasers, more graphene layers (*n* ~2) were used together with a special design of the cavity with w_l(SA) ~30 μm. When considering graphene PQS of ~2.1 μm Ho lasers, one should also take into account that I_S for graphene decreases rapidly with wavelength [31] and it is easier to bleach it at Ho laser wavelengths.

Thus, a general strategy to increase the E_{out} in a compact laser should be an increase of the modulation depth, $\Delta\alpha^*_S$ together with providing conditions for a complete bleaching of the SA. To increase the $\Delta\alpha^*_S$ value, SA based on a multi-layered graphene can be used. However, although the total low-signal absorbance of graphene depends linearly on the number of layers (*n*), the increase of the $\Delta\alpha^*_S$ value occurs much slower due to increasing scattering and, hence, the non-saturable loss. From this point of view, *n* = 2...4 seems to be optimum. An additional benefit from the increase of *n* is the corresponding reduction of I_S [14]. The use of *n* >1 will also lead to further shortening of the Q-switched pulses. To provide tighter focusing in a compact laser, a curved OC placed close to the crystal can be used. ABCD-modeling of the cavity predicts in this case w_l(SA) <40 μm for the Tm:KLuW laser. The losses in the cavity can be further reduced by applying dielectric coatings on the crystal surfaces and the uncoated surface of the substrate of the SA. We believe that this work can open the way to graphene Q-switched 2 μm lasers generating sub-100 ns pulses with energies of few tens of μJ.

4. Conclusion

We present the first passively Q-switched 2-μm microchip laser using Tm:KLuW as an active medium and single layer graphene as a SA. The maximum average output power was 310 mW with a slope efficiency of ~13%. The shortest pulse duration was 285 ns at a repetition rate of 190 kHz. In terms of the achieved short pulse duration and high laser efficiency these results represent a substantial improvement compared to what has already been demonstrated in the existing literature on 2 μm Q-switched lasers applying graphene as a SA (cf. Table 1).

Acknowledgments

This work was supported by the Spanish Government (projects MAT2011-29255-C02-02 and MAT2013-47395-C4-4-R), and by the Generalitat de Catalunya (project 2014SGR1358). F.D. acknowledges also support through the ICREA academia award for excellence in research.